Journal of Biomedical Optics 7(3), 372–377 (July 2002)

# Image reconstruction through turbid media under a transmission-mode microscope

**Xiaosong Gan**
**Min Gu**
Swinburne University of Technology
Centre for Micro-Photonics
School of Biophysical Sciences
and Electrical Engineering
P.O. Box 218 Hawthorn 3122
Victoria, Australia

**Abstract.** In this paper, image enhancement and reconstruction through a turbid medium by utilizing polarization gating and mathematical image reconstruction methods in a microscopic imaging system are investigated. A Monte Carlo simulation model based on Mie theory and the concept of the effective point spread function (EPSF) is adopted to study image formation under a transmission-mode microscope. The results show that polarization gating methods, and particularly the differential polarization gating method, can be efficient in suppressing highly scattered light, which leads to a significant enhancement of image quality. An image reconstruction method based on the concept of the EPSF is demonstrated to be efficient in further improving image quality.  [DOI: 10.1117/1.1483319]

Keywords: polarization; turbid media; Monte Carlo; deconvolution; image reconstruction.

Paper TP-11 received Dec. 18, 2001; revised manuscript received Mar. 27, 2002; accepted for publication Mar. 27, 2002.

## 1 Introduction

Deep tissue imaging has been the focus of the medical imaging world throughout the past decade. The main difficulty involved in imaging through tissue-like turbid media is the multiple scattering effect which greatly degrades the imaging quality. Multiple scattering in a turbid medium causes the randomization of the direction, coherence, and polarization state of an incident light.[1,2] Therefore, optical gating methods, such as coherence gating methods,[3] time gating methods,[4] polarization gating methods,[5–7] confocal microscopy,[8] and other angle gating methods,[9,10] have been proposed and implemented to suppress highly scattered photons. Although optical gating methods have been proven to be efficient in suppressing highly scattered photons and achieved a significant improvement in image resolution, there are fundamental limitations of all the optical gating methods. Due to the fact that only a negligible amount of ballistic and least scattered photons propagate through a thick tissue sample, the signal strength after utilizing optical gating methods may be insufficient to form a high quality image due to the removal of a large amount of highly scattered photons. Under such circumstances, the inverse approach which involves mathematical image processing should be introduced to further improve image resolution.

With the recent development of the effective point spread function (EPSF),[11] image reconstruction based on deconvolution methods can be used to restore image resolution. In this paper, we will demonstrate the efficiency of combined optical gating and image reconstruction methods in improving image quality. It has been proven that polarization gating methods are efficient in improving image resolution in a reflection-mode microscopic imaging system.[12] Therefore, we use polarization gating methods and image reconstruction in a transmission-mode scanning microscope as an example.

This paper is organized as follows. The EPSF under different polarization gating methods is investigated in Sec. 2. In Sec. 3, image resolution of an edge embedded in a turbid medium is evaluated for different polarization gating methods. Section 3 also shows the trade-off between signal strength and image resolution. Image reconstruction is demonstrated in Sec. 4.

## 2 EPSF Under Polarization Gating Methods

The Monte Carlo simulation method we have developed for microscopic imaging through turbid media is based on Mie scattering theory[13,14] and geometric optics. To consider the depolarization of an incident beam propagating through a turbid medium, the Stokes vector method[13,14] can be implemented into the Monte Carlo simulation program. For this purpose, in addition to the spatial coordinates $x$, $y$, $z$, and angular coordinates $\theta$ and $\varphi$, that are used to trace the position and direction of each photon, the Stokes vector is calculated after each scattering event. The detailed description of the simulation model has been reported elsewhere.[12]

Based on the concept of the EPSF, the image intensity $I(\mathbf{r})$ of a thin object can be modeled by the convolution of an object function $o(\mathbf{r})$ and the EPSF $h(\mathbf{r})$[11]

$$I(\mathbf{r}) = \int \int_{-\infty}^{\infty} h(\mathbf{r}')o(\mathbf{r}-\mathbf{r}')d\mathbf{r}' = h(\mathbf{r}) \otimes_2 o(\mathbf{r}), \quad (1)$$

where $\otimes_2$ denotes the two-dimensional convolution process, and $\mathbf{r}=(x,y)$ is the transverse coordinate. Forty million illumination photons have been used in the Monte Carlo simulation to ensure the accuracy of an EPSF for a transmission-mode scanning optical microscope.

A schematic diagram of a transmission-mode scanning microscope is shown in Figure 1. $L_1$ and $L_2$ are, respectively, the

Address all correspondence to Xiaosong Gan. Tel.: 61-3-921-48675; Fax: 61-3-92145435; E-mail: xgan@swin.edu.au

1083-3668/2002/$15.00 © 2002 SPIE

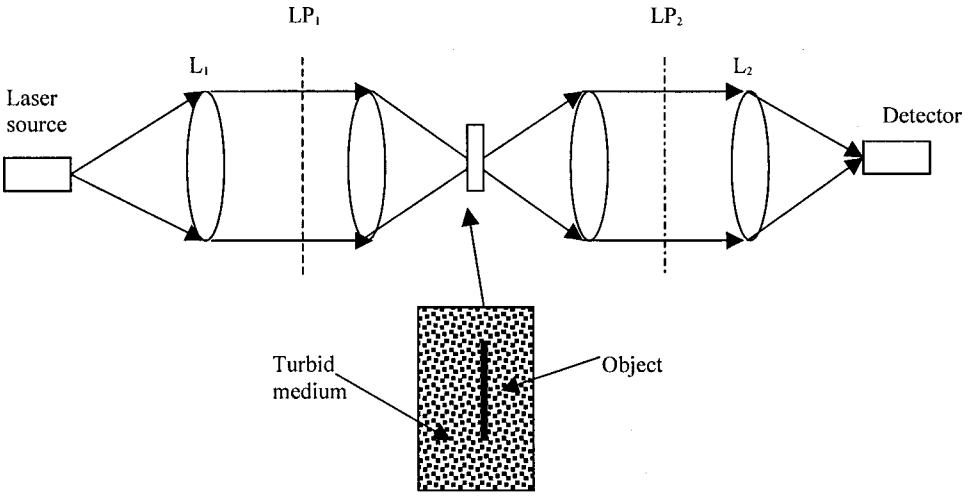


**Fig. 1** A schematic diagram of a transmission-mode scanning optical microscope.

illumination and detection objectives. A polarizer $LP_1$ is placed in the illumination path to produce a linearly polarized beam, and an analyzer $LP_2$ is placed in the detection path. The degree of polarization $\gamma$ of the light passing through a turbid medium is defined as

$$\gamma = \frac{I_p - I_s}{I_p + I_s}, \tag{2}$$

where $I_p$ and $I_s$ are, respectively, the light intensity detected with the analyzer parallel and perpendicular to the direction of the polarizer.

Consider a turbid slab, illuminated by an objective ($L_1$ in Figure 1) of numerical aperture ($NA$) 0.25. Assume that $L_1$ and $L_2$ are identical. The turbid medium consists of polystyrene beads ($n=1.59$) suspended in water ($n=1.33$). Two types of polystyrene beads of diameters 0.35 and 0.48 $\mu$m are used as scattering particles in the turbid medium, respectively. The anisotropy values $g$ corresponding to 0.35 and 0.48 $\mu$m polystyrene beads are 0.72 and 0.81, respectively, for a He–Ne laser at wavelength 0.633 $\mu$m.[13,14] The scattering mean free path length $l_s$, is assumed to be 20 $\mu$m for all cases and the thickness of the turbid slab is considered as twice the focal depth $d$. In this paper, theoretical modeling of image formation under polarization gating method and image reconstruction of an object embedded in such a turbid medium is investigated in detail.

The degree of polarization as a function of focal depth is shown in Figure 2. It is noticed that for a turbid medium consisting of small scattering particles, the depolarization of the scattered light is faster than that for large scattering particles. For example, at the depth of 100 $\mu$m, the degree of polarization drops to 9% and 28% for a turbid medium consisting of 0.35 and 0.48 $\mu$m beads, respectively. The speed of depolarization is related to the anisotropy value $g$, which reflects a directional change of photon propagation after each scattering event. For small particles, the directional change of a scattered photon is large at each scattering event due to the small value of $g$, which results in a more significant change in the polarization state of the scattered light.

The EPSFs at the depth of 100 $\mu$m in the medium consisting of 0.48 $\mu$m beads under different polarization gating methods are shown in Figure 3. The results show an improvement of image resolution under polarization gating methods. The improvement is not only reflected on the narrowing of the EPSF under polarization gating methods, but also the significant reduction of the tail of the EPSF, which indicates an

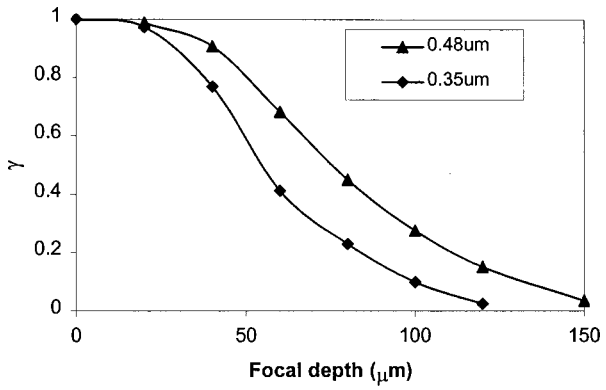


**Fig. 2** Degree of polarization $\gamma$ as a function of the focal depth $d$.

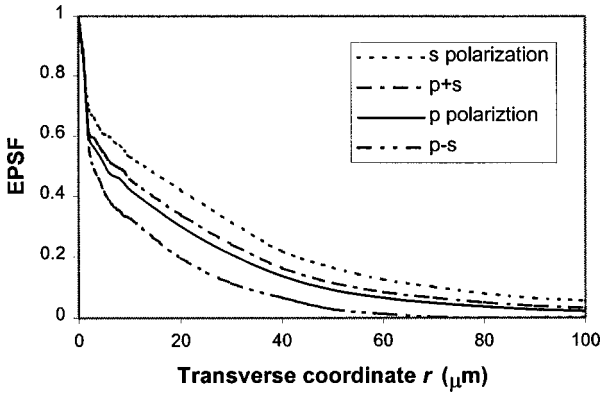


**Fig. 3** EPSF at the focal depth $d$ of 100$\mu$m in a turbid medium consisting of 0.48 $\mu$m beads.

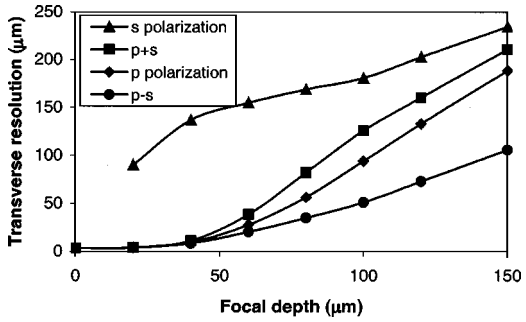


**Fig. 4** Image resolution as a function of the focal depth $d$ for an edge embedded in a turbid medium consisting of 0.48 $\mu$m beads.

efficient suppression of highly scattered photons. It should also be pointed out that the improvement is particularly significant under the differential polarization gating method.

## 3 Image Resolution and Signal Level with Polarization Gating Methods

In order to characterize image resolution, we assume that a high absorption edge object is embedded in the middle of a scattering slab scanned in the $x$ direction. From the image intensity of the sharp absorption edge, the transverse resolution, $\Gamma$, is defined as the distance between the 90% and 10% intensity points.[12]

The transverse resolution as a function of the focal depth in a medium consisting of 0.48 $\mu$m beads is illustrated in Figure 4 for different polarization gating methods. $\Gamma_p$ and $\Gamma_s$ are, respectively, the transverse resolution obtained with the analyzer parallel and perpendicular to the polarizer. $\Gamma_{p-s}$ and $\Gamma_{p+s}$ are, respectively, the transverse resolution obtained with the differential polarization gating method and without any polarization gating method. It is shown that $\Gamma_{p-s}$ is better than $\Gamma_p$ and that the differential polarization gating method offers the highest resolution among all. This feature can be understood from the difference in the degree of polarization between unscattered and scattered photons. Since unscattered and/or less scattered photons have a higher degree of polarization than multiply scattered photons (Figure 2), more contribution from these photons can be ensured in forming an image through the use of the polarization gating methods. The weighting of the scattered photons can be reduced accordingly by utilizing polarization gating methods, which leads to high resolution when the parallel and differential polarization gating methods are used (Figure 4). It is noticed from Figure 4 that the difference of transverse resolution between $\Gamma_p$ and $\Gamma_s$, under two polarization states $p$ and $s$, decreases with increasing the focus depth $d$. When $\gamma \rightarrow 0$, the two curves representing $\Gamma_p$ and $\Gamma_s$ move toward each other. Because of the difference of the transverse resolution between the two orthogonal states of polarization becomes less pronounced, the resolution improvement by utilizing polarization gating methods becomes less effective.

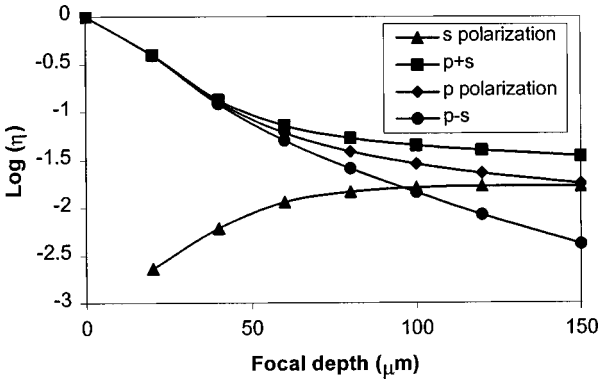


**Fig. 6** Signal level as a function of the focal depth $d$ in a turbid medium consisting of 0.48 $\mu$m beads.

The transverse resolution as a function of the focal depth in a medium consisting of 0.35 $\mu$m beads is illustrated in Figure 5. The improvement of the transverse resolution under polarization gating methods is similar to what has been demonstrated in a turbid medium with large scatterers (Figure 4). However, it is noticed that the differential polarization gating method is only valid up to the focal depth of 120 $\mu$m. Because of the fast depolarization speed for small scatterers, the collected signal at the focal depth larger than 120 $\mu$m becomes totally unpolarized. Therefore, no differential image can be measured beyond this focal depth.

Figure 6 shows the dependence of the measured signal

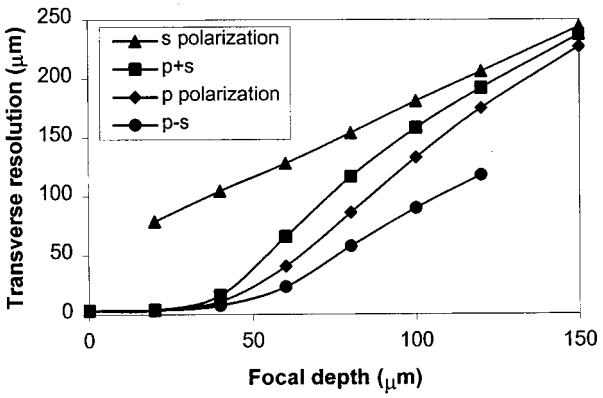


**Fig. 5** Image resolution as a function of the focal depth $d$ for an edge embedded in a turbid medium consisting of 0.35 $\mu$m beads.

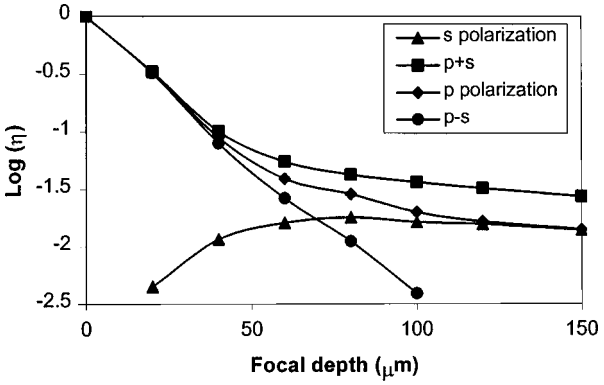


**Fig. 7** Signal level as a function of the focal depth $d$ in a turbid medium consisting of 0.35 $\mu$m beads.

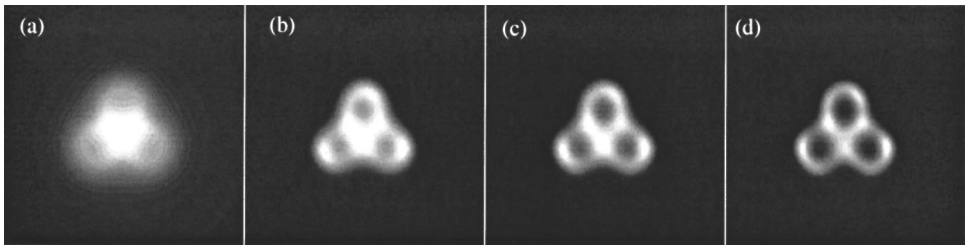


**Fig. 8** Reconstruction of images without polarization gating methods: (a) before restoration; (b) after 100 iterations; (c) after 200 iterations; (d) after 400 iterations.

level on the sample thickness $d$ in a medium consisting of 0.48 $\mu$m beads under different polarization gating methods. The signal level $\eta$ has been normalized by the signal measured without the turbid medium ($d=0$) and any polarization gating methods. It is noticed that the reduction in the signal level under parallel polarization gating is insignificant. However, the reduction in the signal level under differential polarization becomes significant when $\gamma \rightarrow 0$, which indicates the collect light becomes totally unpolarized. The signal level as a function of the focal depth $d$ for a turbid medium with small scatterers (0.35 $\mu$m beads) is illustrated in Figure 7. The comparison between Figures 6 and 7 shows that at a given focal depth, the signal strength, especially the signal strength under the differential polarization gating method, is lower in a turbid medium with small scatterers. For example, at the focal depth of 100 $\mu$m, the signal strength is five times higher in a turbid medium consisting of 0.48 $\mu$m beads than that in a turbid medium consisting of 0.35 $\mu$m beads. This is due to the faster depolarization effect in a turbid medium with smaller scatterers.

## 4 Image Reconstruction with Polarization Gating Methods

As shown in the last sections, polarization gating methods can play an important role in microscopic imaging through turbid media. However, there are some limitations of polarization gating methods, for example, when $\gamma \rightarrow 0$, the improvement by utilizing polarization gating methods becomes less pronounced. It has also been demonstrated that signal strength can be insufficient if a significant amount of scattered photons is removed. It is worthwhile to discuss the role of scattered photons. Are multiple scattered photons merely noise and make no positive contribution in building an image? The statistical analysis of scattered photon distribution shows that scattered photons still carry information about embedded objects.[15] However, they are always treated as noise when high resolution is pursued. In a thick turbid medium, because of the nearly nonexistence of ballistic or least scattered photons, multiple scattered photons have to be taken into account in building up an image. This inevitably degrades the image resolution. Under this circumstance, the inverse approach (image reconstruction) is regarded as the solution to the problem. Here we use the expectation-maximization (EM) algorithm for maximum-likelihood image restoration.[16] The most basic form of the EM algorithm can be expressed as follows:[17]

$$I^k(\mathbf{r}) = h(\mathbf{r}) \otimes_2 s^k(\mathbf{r}), \tag{3}$$

where $I^k(\mathbf{r})$ and $s^k(\mathbf{r})$ are, respectively, the image intensity and the estimated object function at $k$th iteration. The initial estimated object function $s^0(\mathbf{r})$ used in the deconvolution process is the original image. The predicated image intensity $I^k(\mathbf{r})$ is compared with the recorded image intensity

$$d^k(\mathbf{r}) = I(\mathbf{r}) / I^k(\mathbf{r}). \tag{4}$$

The ratio $d^k(\mathbf{r})$ is then projected back to the object space with a normalization factor $H(0)$

$$r^k(\mathbf{r}) = h(-\mathbf{r}) \otimes_2 d^k(\mathbf{r}) / H(0), \tag{5}$$

where $r^k(\mathbf{r})$ is a correction factor, and the normalization factor $H(0)$ is derived as the two-dimensional integration of the EPSF. The estimated image intensity of the next iteration can be derived as

$$I^{k+1}(\mathbf{r}) = I^k(\mathbf{r}) \times r^k(\mathbf{r}). \tag{6}$$

Here we design an object which consists of three rings. Each ring has an outer radius of 20 $\mu$m and an inner radius of 15 $\mu$m. Such an object emulates a biological cell cluster, and the deconvolution process of this object is demonstrated in

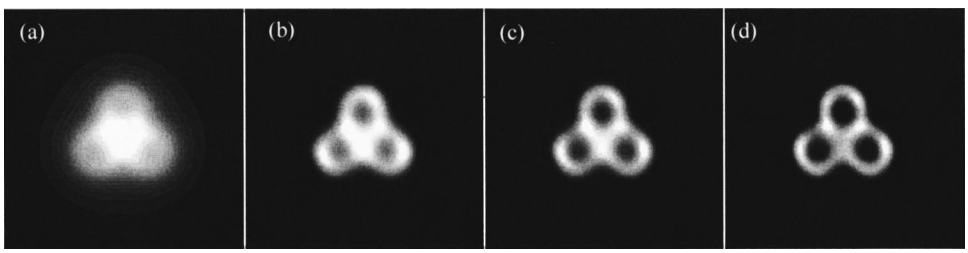


**Fig. 9** Reconstruction of images under parallel polarization gating methods: (a) before restoration; (b) after 100 iterations; (c) after 200 iterations; (d) after 400 iterations.

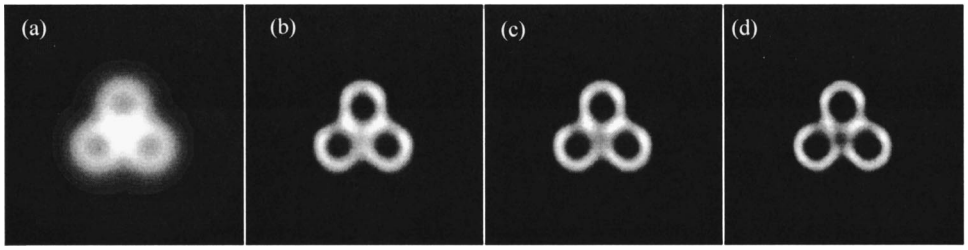


**Fig. 10** Reconstruction of images under differential gating methods: (a) before restoration; (b) after 100 iterations; (c) after 200 iterations; (d) after 400 iterations.

Figure 8. Here we use the image at $d=120\ \mu$m depth and without any polarization gating method as an example. The turbid medium consists of 0.48 $\mu$m beads. Before the deconvolution process, the image is blurred and the ring structure is totally washed out by the blurring effect. It is shown that the image resolution loss due to multiple scattering can be partially recovered through the image reconstruction process. After 200 iterations, the ring structure starts to re-emerge; however, the ring structure is still quite blurred and the three ring structures cannot be resolved from each other [Figure 8(b)]. With more iterations, blurring on the ring structure becomes less significant [Figures 8(c) and 8(d)], and there is also a slight indication of resolving three rings after 400 iterations [Figure 8(d)]. It should be pointed out that the EPSF is not only much broader compared with a normal PSF, but also has a significant tail that can affect the image formed (Figure 2). Therefore, the cutoff of the EPSF used for deconvolution process needs to be carefully determined.

The deconvolution process of this object under parallel and differential polarization gating methods is shown in Figures 9 and 10, respectively. Because some scattered photons have been removed by the optical gating effect, the images before the deconvolvution process are better under parallel and differential gating methods, with the best image produced under the differential gating method. Under the parallel polarization gating method, the improvement in image quality is limited, since the amount of scattered photons removed is insignificant. Therefore the deconvolution process on the image recorded under the parallel polarization gating method has a very similar effect compared with that without optical gating methods. For example, the images after 100, 200, and 400 iterations are only slightly better, compared with those respective images recorded without polarization gating methods (Figure 9).

The combination of the differential polarization gating and the image reconstruction methods produces the images with the best quality. It is noticed in Figure 10(a) that the three ring structures can be vaguely identified even before the deconvolution process, which indicates that the image has been improved significantly through the differential polarization gating method, due to the removal of a large amount of highly scattered photons. After only 100 iterations, each ring structure can be clearly identified [Figure 10(b)]. After 400 iterations, not only can the three ring structure be resolved, but also the width of each ring becomes thinner and approaches its original width [Figure 10(d)]. This phenomenon shows that with the differential polarization gating method, the deconvolution process can be more efficient.

The comparison of reconstructed images after 1000 iterations under different gating situations is shown in Figure 11. It is demonstrated that with a stronger gating effect, the better reconstructed images can be obtained. It is shown that the width of the rings in Figure 11(c) is only 6 $\mu$m, which is close to the actual width (5 $\mu$m) of the object. The comparison of the images in Figure 11 and their respective images after 400 iterations shows that the images after 400 and 1000 iterations are very similar in terms of the width of the rings. This indicates that the rate of convergence becomes significantly small, and that the image will not be further improved through more iterations.

## 5 Conclusion

Polarization gating methods, including the parallel polarization gating and differential polarization gating methods, in microscopic imaging through a turbid medium have been studied in this paper. The results show that the polarization gating methods, particularly the differential polarization gat-

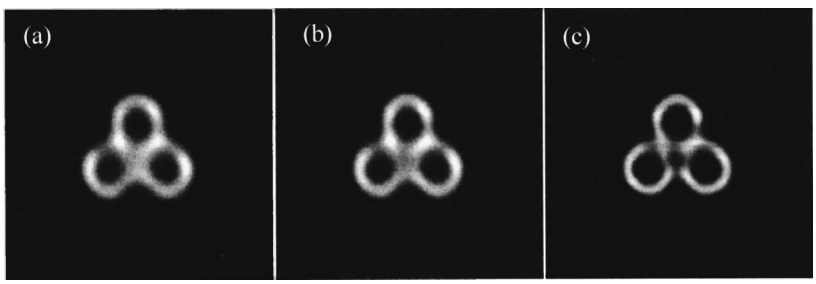


**Fig. 11** The comparison of reconstructed images after 1000 iterations: (a) without polarization gating methods; (b) under the parallel polarization method; (c) under the differential polarization gating method.

ing method, are efficient in improving image resolution. It is also demonstrated that signal strength under differential polarization gating drops quickly when the collected signal becomes totally depolarized.

Another important result is that the combination of polarization gating and image reconstruction methods offers a further improvement in image resolution. The differential polarization gating method not only provides the best images before the mathematical reconstruction, but also makes the reconstruction process more efficient in recovering the loss of imaging resolution.

## Acknowledgment

The authors thank the Australian Research Council for its support.

## References

1. J. G. Fujimoto, S. De Silvestri, E. P. Ippen, C. A. Puliafito, R. Margolis, and A. Oseroff, ''Femtosecond optical ranging in biological systems,'' *Opt. Lett.* **11**, 150–153 (1986).
2. S. T. Flock, B. C. Wilson, and M. S. Patterson, ''Total attenuation coefficients and scattering phase functions of tissues and phantom materials at 633 nm,'' *Med. Phys.* **14**, 835–841 (1987).
3. M. Toida, M. Kondo, T. Ichimura, and H. Inaba, ''Two-dimensional coherent detection imaging in multiplescattering media based on the directional resolution capability of the optical heterodyne method,'' *Appl. Opt.* **52**, 391–394 (1991).
4. S. L. Jacques, ''Time resolved propagation of ultrashort laser pulses within turbid tissue,'' *Appl. Opt.* **28**, 2223–2229 (1989).
5. J. M. Schmitt, A. H. Gandjbakhche, and R. F. Bonner, ''Use of polarization light to discriminate short path photons in a multiply scattering medium,'' *Appl. Opt.* **31**, 6535–6546 (1992).
6. S. P. Morgan, M. P. khong, and M. G. Somekh, ''Effects of polarization state and scatter concentration on optical imaging through scattering media,'' *Appl. Opt.* **36**, 1560–1565 (1997).
7. S. Schilders, X. Gan, and M. Gu, ''Resolution improvement in microscopic imaging through turbid media based on differential polarization-gating,'' *Appl. Opt.* **37**, 4300–4302 (1998).
8. X. Gan, S. P. Schilders, and M. Gu, ''Image formation in turbid media under a microscope,'' *J. Opt. Soc. Am. A* **15**, 2052–2058 (1998).
9. S. Schilders, X. Gan, and M. Gu, ''Microscopic imaging through turbid media by use of annular objective for angle-gating,'' *Appl. Opt.* **37**, 5320–5326 (1998).
10. M. Gu, T. Tannous, and C. J. R. Sheppard, ''Effect of an annular pupil on confocal imaging through highly scattering media,'' *Opt. Lett.* **21**, 312–314 (1996).
11. X. Gan and M. Gu, ''Effective point-spread function for fast image modeling and processing in microscopic imaging through turbid media,'' *Opt. Lett.* **24**, 741–743 (1999).
12. X. Gan, S. P. Schilders, and M. Gu, ''Image enhancement through turbid media under a microscope by use of polarization gating methods,'' *J. Opt. Soc. Am. A* **16**, 2177–2184 (1999).
13. M. Born and E. Wolf, *Principles of Optics*, Oxford, Pergamon, New York (1980).
14. C. F. Bohern and D. R. Huffman, *Absorption and Scattering of Light by Small Particles*, Wiley, New York (1983).
15. X. Gan, S. P. Schilders, and M. Gu, ''Image formation in turbid media under a microscope,'' *J. Opt. Soc. Am. A* **15**, 2052–2058 (1998).
16. T. J. Holmes, ''Maximum-likelihood image restoration adapted for non-coherent optical imaging,'' *J. Opt. Soc. Am. A* **5**, 666–673 (1988).
17. J. A. Conchello and E. W. Hansen, ''Enhanced 3-D reconstruction from confocal scanning microscope images: deterministic and maximum likelihood reconstruction,'' *Appl. Opt.* **29**, 3795–3804 (1990).